9. R. V. Parthasarathy and C. R. Martin, *ibid.* **369**, 298 (1994).
10. Y. Shinohara *et al.*, *J. Biochem.* **117**, 1076 (1995).
11. J. J. Hickman, D. Ofer, P. E. Laibinis, G. M. Whitesides, M. S. Wrighton, *Science* **252**, 688 (1991).
12. H. M. McConnell *et al.*, *ibid.* **257**, 1906 (1992).
13. A. Brecht and G. Gauglitz, *Biosens. Bioelectron.* **10**, 923 (1995).
14. W. Göpel *et al.*, Eds., *Sensors Update* (Wiley-VCH, Weinheim, Germany, 1989–1996), vols. 1–9.
15. V. V. Doan and M. J. Sailor, *Science* **256**, 1791 (1992).
16. B. Rossi, *Optics* (Addison-Wesley, Reading, MA, 1957).
17. Optically flat thin films of PSi were prepared by electrochemical etch of polished (100)-oriented *p*-type Si (B-doped, 3 ohm-cm resistivity) in a 1:1 98% ethanol:49% aqueous HF solution for 2 min at a current density of 50 mA/cm^2. Scanning electron microscopy and atomic force microscopy showed that PSi films prepared in this manner are 1 to 5 μm thick and contain pores with diameters up to 200 nm. The PSi matrix was modified by Br_2(g) oxidation in an evacuated chamber for 1 hour followed by hydrolysis in air.
18. For attachment of DNA, we synthesized a trimethoxy-3-bromoacetamidopropylsilane linker by reaction of bromoacetic acid with 1-(3-dimethylaminopropyl)-3-ethylcarbodiimide hydrochloride in CH_2Cl_2 solution. The linker product was purified by column chromatography on silica gel and characterized by ^{1}H nuclear magnetic resonance spectroscopy. The oxidized PSi samples were then exposed to a toluene solution of the linker for 2 hours. The sample was thoroughly rinsed with pure toluene and CH_2Cl_2 and dried overnight in vacuum. A purified (high-performance liquid chromatography) 5′-phosphorothiate oligonucleotide (DNA-A) (5′-pGC CAG AAC CCA GTA GT-3′) (236 μg, 47.7 nmol) was dissolved in a solution of (1:1:0.2 water/dimethyl-formamide/5% $NaHCO_3$(aq); pH 8.5) and the linker-derivatized PSi chip was immersed in the DNA solution for 2 hours. The presence of the DNA modification on the PSi surface (DNA-A) was confirmed by Fourier transfer infrared spectroscopy.
19. A. Brecht and G. Gauglitz, in *Frontiers in Biosensorics II: Practical Applications*, F. W. Scheller *et al.*, Eds. (Birkhäuser, Basel, Switzerland, 1997), pp. 1–16.
20. We prepared a linker with attached biotin by reaction of iodoacetyl-LC-biotin (Pierce Biochemicals) with 3-mercaptopropyltrimethoxysilane (Aldrich Chemicals) in dimethylformamide. After purification, the biotinylated linker was dissolved in ethanol or dimethylformamide, and the oxidized PSi sample was immersed in the solution for 12 hours. The sample was then rinsed thoroughly with ethanol and dried under a stream of N_2.
21. B. R. Hemenway, O. Solgard, D. M. Bloom, *Appl. Phys. Lett.* **55**, 349 (1989).
22. I. Schechter, M. Ben-Chorin, A. Kux, *Anal. Chem.* **67**, 3727 (1995).
23. D. Stievenard and D. Deresmes, *Appl. Phys. Lett.* **67**, 1570 (1995).
24. A. Motohashi *et al.*, *Jpn. J. Appl. Phys.* **35**, 4253 (1996).
25. K. Watanabe, T. Okada, I. Choe, Y. Sato, *Sens. Actuators B* **33**, 194 (1996).
26. C. Kittel, *Introduction to Solid State Physics* (Wiley, New York, ed. 6, 1986).
27. D. R. Neu, J. A. Olson, A. B. Ellis, *J. Phys. Chem.* **97**, 5713 (1993).
28. A. J. Bard and L. R. Faulkner, *Electrochemical Methods: Fundamentals and Applications* (Wiley, New York, 1980).

29. Financial support was provided by the Office of Naval Research (N000149511293) through the Multi-Disciplinary University Research Initiative of the Department of Defense. We thank J. E. Kyte and R. C. Dynes for helpful discussions. M.R.G. thanks the Scripps Research Institute for matching equipment funds. V.S.-Y.L. was supported under a Skaggs Institute postdoctoral fellowship, K.M. under an NIH postdoctoral fellowship (GM18309), and K.S.D. under an NIH predoctoral fellowship (2SO6 GM47165-06).

*7 July 1997; accepted 23 September 1997

Quasi–Phase-Matched Third-Harmonic Generation in a Quasi-Periodic Optical Superlattice

Shi-ning Zhu,* Yong-yuan Zhu,* Nai-ben Ming*†

Quasi-periodic structure can be introduced into nonlinear optical materials such as $LiTaO_3$ crystals. Such structures were used for quasi–phase-matching second-harmonic generation. These materials are now shown to be able to couple second-harmonic generation and sum-frequency generation through quasi–phase-matching. The approach led to a direct third-harmonic generation with high efficiency through a coupled parametric process. The result verifies that high-order harmonics may be generated in a quadric nonlinear medium by a number of quasi–phase-matching processes, and therefore, exhibits a possible important application of quasi-periodic structure materials in nonlinear optics.

In dielectric crystals, the most important physical processes are the propagation and excitation of classical waves (optical and ultrasonic waves). The behavior of classical waves in a homogeneous dielectric crystal is the same as that in a continuous medium, because the wave vector of a classical wave is much smaller than the reciprocal vectors of crystal lattice. However, if some microstructure is introduced into a dielectric crystal, forming a superlattice, and if the reciprocal vectors of the superlattice are comparable with the classical wave vectors, the situation is quite different. The propagation of classical waves in a superlattice (classical system) is similar to the electron motion in a periodic potential of crystal lattice (quantum system). Thus, some ideas in solid-state electronics—for example, the reciprocal space, Brillouin zone, dispersion relation, and the like—may be used in classical wave processes. Such is the case for photonic band-gap materials (*1*). With classical systems, eigenvalues and eigenfunctions were measured directly (*2*). These are difficult if not impossible to obtain in quantum systems. On the other hand, the interactions between wave vectors of classical waves and reciprocal vectors of the superlattice may generate some new physical effects. In nonlinear optical fields, the interactions have led to new laser frequency generations in quasi–phase-matching (QPM) schemes from a number of optical superlattice crystals such as $LiNbO_3$, $LiTaO_3$, and $KTiOPO_4$ (*3*, *4*).

The above concepts may be equally applied to the quasiperiodic structure. Despite the large amount of research on the quasiperiodic structure since its discovery in 1984 (*5*), whether this kind of structure can be of any practical use remains undetermined. It was proposed that the quasi–phase-matching theory can be extended from periodic structures to quasiperiodic structures (*6*), which may find applications in nonlinear optics through the QPM method. With the development of the electric poling technique, ferroelectric crystals such as $LiTaO_3$, $LiNbO_3$, $KTiOPO_4$, and the like with quasiperiodically domain-inverted structure (hereafter we call it quasiperiodic optical superlattice, or QPOS) can be fabricated. We previously reported the experimental results of multiwavelength second-harmonic generation (SHG) in a Fibonacci QPOS $LiTaO_3$ (*6*). Because more reciprocal vectors can be provided by a QPOS, not only the quasi–phase-matched (QPM) multiwavelength SHG but also some coupled parametric processes, such as the third-harmonic generation (THG) and fourth-harmonic generation, can be realized with high efficiency. Taking THG as an example, we present our results using the second-order nonlinear optical processes in a QPOS $LiTaO_3$ crystal.

THG has a wide application as a means to extend coherent light sources to short wavelengths. The creation of the third harmonic directly from a third-order nonlinear process is of little practical importance because of the intrinsic low third-order optical nonlinearity. Conventionally, an efficient THG was achieved by a two-step process. Two nonlinear optical crystals are needed: the first one for SHG and the second one for sum-frequency generation (*7*). In this regard, QPOS has some advantages over the conventional method. Here, only one crystal is needed and the harmonic generation can be realized with high efficiency by using the largest nonlinear optical coefficient over the entire transparency range of the material.

A QPOS may be thought to contain two

National Laboratory of Solid State Microstructures, Nanjing University, Nanjing 210093, China, and Center for Advanced Studies in Science and Technology of Microstructures, Nanjing 210093, China.

*These authors contributed equally to this work.
†To whom correspondence should be addressed.

or more linear independent periods, whose ratios are given by irrational numbers (8). Its reciprocal vectors are indexed by two or more integers, which is different from a periodic structure's reciprocal G_n indexed by one integer. For a Fibonacci QPOS, the QPM conditions for THG in a colinear interaction are

$$\Delta k_1 = k_2 - 2k_1 - G_{m,n} = 0 \quad (1)$$

for SHG and

$$\Delta k_2 = k_3 - k_2 - k_1 - G_{m',n'} = 0 \quad (2)$$

for sum-frequency generation process, respectively, where k_1, k_2, and k_3 are the wave vectors of the fundamental, second-, and third-harmonic fields, respectively; $G_{m,n}$ and $G_{m',n'}$ are predesigned two different reciprocal vectors of the superlattice.

The QPOS used here consists of two fundamental blocks, *A* and *B*, arranged according to the Fibonacci sequence: *ABAABABAABAAB* . . . (*9*). For $LiTaO_3$, each block (*A* or *B*) contains a pair of antiparallel 180° domains. The widths of *A* and *B* are l_A and l_B, respectively, where $l_A = l_{A1} + l_{A2}$ and $l_B = l_{B1} + l_{B2}$. We assumed that $l_{A1} = l_{B1} = l$ for the width of the positive domain, and $l_{A2} = l(1 + \eta)$, and $l_{B2} = l(1 - \tau\eta)$ for the width of the negative domain. Here, l and η are two adjustable structure parameters and $\tau = (1 + \sqrt{5})/2$ is the golden ratio (Fig. 1A). The reciprocal vector $G_{m,n} = 2\pi D^{-1}(m + n\tau)$, where $D = \tau l_A + l_B$ is an "average structure parameter." Theoretically, $l = sl_{c2} = \nu l_{c3}$, where l_{c2} and l_{c3} are, respectively, the coherence length of SHG and the sum-frequency generation in a homogeneous crystal and where s = 1, 3, 5, and so on, and $\nu = \tau, \tau^2, \tau^3$, and so on. When l is fixed, the variation of η can be used to adjust the magnitude of the effective nonlinear coefficient to obtain the most efficient THG (6).

The QPOS was fabricated by quasi-periodically poling a *z*-cut $LiTaO_3$ wafer at room temperature (*10*). The structure parameters were selected to be: $l = l_{c2} = \tau^2 l_{c3} = 10.7$ μm and $\eta = 0.23$, so that block *A* and *B* were 24 μm and 17.5 μm in width, respectively. The quasi-periodic structure can be confirmed by observing the etched *y* surface of the sample (Fig. 1C). It consisted of 13 generations and had a total length of ~8 mm. The sample thickness was 0.5 mm. In this design, the reciprocal vector $G_{1,1}$ was used for QPM SHG, whereas $G_{2,3}$ was used for QPM sum-frequency generation. Here, the two processes no longer proceed alone but couple each other. This coupling led to a continuous energy transfer from fundamental to second- to third-harmonic fields, thus, a direct third-harmonic was generated from the QPOS with high efficiency (Fig. 1D).

THG was tested with a tunable optical parametric oscillator pumped with an yttrium-aluminum-garnet laser (Nd-YAG, NY81-10, Continuum, Santa Clara, California) with a pulsewidth of 8 ns and a repetition rate of 10 Hz. The linewidth of the fundamental wave was about 1.5 nm at 1.6 μm. In order to use the largest nonlinear optical coefficient d_{33} of $LiTaO_3$, the fundamental wave was *z*-polarized and propagated along the *x* axis of the sample (Fig. 1B). It was weakly focused and coupled into the polished end of the sample. For the system, the confocal parameter $Z_0 = 2$ cm, and the radius of the waist spot inside the sample was $\varpi_0 = 30$ μm. When the fundamental wavelength was tuned to 1.570 μm, green light at 0.523-μm wavelength was generated from the sample (Fig. 2). The third-harmonic peak has a shift of 1.5 nm to the theoretical value calculated from the dispersion relation of bulk $LiTaO_3$ at room temperature (25°C). A green light of 6 mW was obtained for an average fundamental power of 26 mW (with an average power density ~1 kW/cm^2). The conversion efficiency was close to 23%. Together with the THG, an SHG was observed in the same range of fundamental wavelength. The output of SHG and THG were stable, and no optical damage was observed at this fundamental intensity level. The second- and third-harmonic tuning curves, calculated [according to (6)] and measured, are shown in Fig. 3, A and B, respectively. The measured peak shifts and widening from calculated values may arise from some uncertainties in the Sellmeier equation used to estimate the dependence of the refractive index on wavelength. A focused fundamental beam with wide linewidth was used, and

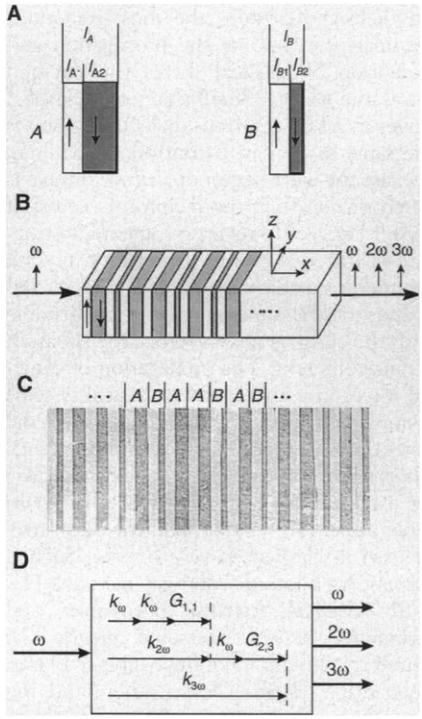

Fig. 1. QPOS made from a single $LiTaO_3$ crystal. The arrows indicate the directions of spontaneous polarization. (**A**) Two building blocks, *A* and *B*, each composed of one positive and one negative ferroelectric domain. (**B**) Schematic diagram shows a QPOS composed of two blocks, *A* and *B*, arranged in Fibonacci sequence and the polarization orientation of electric fields in the THG process with respect to the superlattice. (**C**) Optical micrograph shows a QPOS of a single $LiTaO_3$ crystal revealed by etching. (**D**) Schematic diagram of the process of THG in a QPOS material. The QPOS has two specially designed reciprocal vectors: $G_{1,1}$ is used to compensate the mismatch of wave vectors in the SHG process, and $G_{2,3}$ is used to compensate the mismatch of wave vectors in the SFG process. Two QPM conditions, $\Delta k_1 = 0$ and $\Delta k_2 = 0$, are simultaneously satisfied in the coupled parametric process, which leads to a THG with high efficiency.

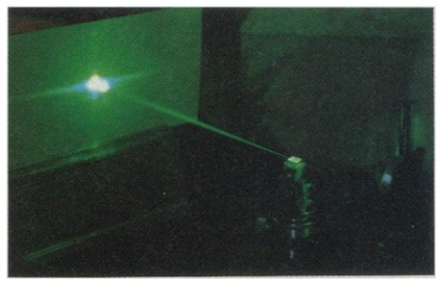

Fig. 2. A third-harmonic beam of green light was generated when an infrared light from an optical parametric oscillator passed through a 8-mm-long QPOS $LiTaO_3$ crystal.

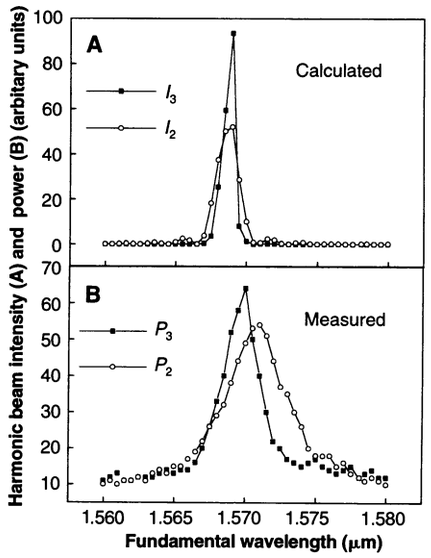

Fig. 3. The SHG and THG tuning curves for the QPOS sample, (**A**) calculated and (**B**) measured by using an *ns*-optical parametric oscillator.

some imperfections in the domain pattern could also widen the bandwidth.

Figure 4A shows the dependence of second- and third-harmonic average power on the fundamental average power measured at the output end of the sample. I_3 grows slower than I_2 when I_1 is low (Fig. 4A). With the increase of I_1, the increase rate of I_3 grows faster, whereas that of I_2 becomes slower, because more and more I_2 participates in the sum-frequency process. Finally, I_3 approaches and even exceeds I_2. These results imply a coupling effect of three waves when the phases are matched. The situation continues until conversion efficiency exceeds a certain level under which a nondepletion approximation will be no longer valid.

The THG process can be analyzed by solving the coupled nonlinear equations that describe the interaction of the three fields E_ω, $E_{2\omega}$, and $E_{3\omega}$ in QPOS. We can get an analytical result for boundary conditions $E_{2\omega}(0) = 0$ and $E_{3\omega}(0) = 0$. Under small signal approximation and QPM conditions (*11*), the second- and third-harmonic intensities are

$$I_2 = \frac{8\pi^2 d_{m,n}^2 L^2}{n_1^2 n_2 c \varepsilon_0 \lambda^2} I_1^2 \qquad (3)$$

and

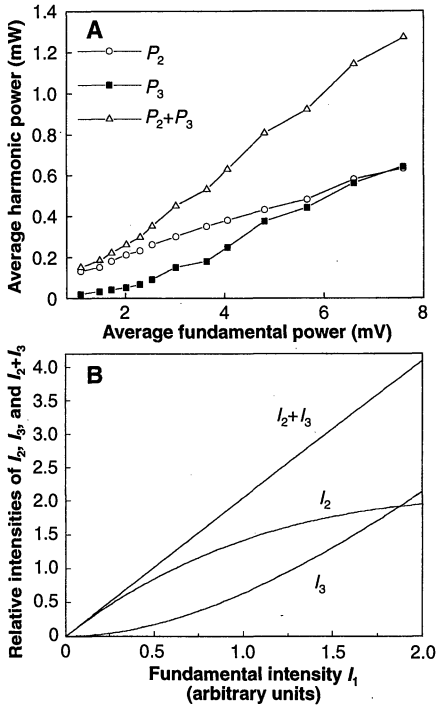

Fig. 4. (**A**) The average powers of second- and third-harmonic fields versus the average power of the fundamental field for the QPOS sample. The light source is an *ns*-optical parametric oscillator with a repetition of 10 Hz. (**B**) The calculated relative intensities of I_2, I_3, and $I_2 + I_3$ versus fundamental intensity I_1.

$$I_3 = \frac{144\pi^4 d_{m,n}^2 d_{m',n'}^2 L^4}{n_1^3 n_2^2 n_3 c^2 \varepsilon_0^2 \lambda^4} I_1^3 \qquad (4)$$

with the effective nonlinear coefficient $d_{m,n} = d_{1,1}$ and $d_{m',n'} = d_{2,3}$ (6). Here, n_1, n_2, and n_3 represent the refraction indices of the fundamental, second, and third harmonics, respectively; c is the speed of light in a vacuum; λ is the fundamental wavelength; and ε_0 is the dielectric constant of vacuum. From Eqs. 3 and 4 it is evident that I_3 would depend more strongly on the fundamental intensity I_1 and the length of sample L than I_2. The theoretical results according to Eqs. 3 and 4 (Fig. 4B) are in excellent agreement with the experimental ones (Fig. 4A).

The result obtained here can be compared with that from a third-harmonic generator constructed by two periodic superlattices, each with a length $L/2$. The second harmonic is generated in the first superlattice with period Λ_1, using the first-order QPM; it then mixes with the fundamental wave in the second superlattice with period Λ_2, using the third-order QPM (if a first-order QPM is used in sum-frequency process, the grating period is too small to fabricate a bulk sample with the thickness of 0.5 mm by poling). Compared with the two-step process, the conversion efficiency in a QPOS is increased by a factor of

$$\frac{d_{1,1}^2 d_{2,3}^2 L^4}{d_1^2 d_3^2 \left(\frac{L}{2}\right)^2 \left(\frac{L}{2}\right)^2} \cong 8 \qquad (5)$$

Here, $d_{1,1} \approx 0.86 d_1$ and $d_{2,3} \approx 0.88 d_3$, where d_1 and d_3 are the effective nonlinear coefficients of SHG and sum-frequency generation of two periodic superlattices, respectively (6). The reason for this is that in the traditional two-step scheme, second-harmonic and sum-frequency processes are not coupled and achieved in two separate steps, respectively. Therefore, its effective interaction length is only one-half of a QPOS with the same total length where two processes are coupled.

The Fibonacci QPOS is only a subclass of quasi-periodic structures, and $LiTaO_3$ is a ferroelectric. In fact, the quasi-periodic structure can be extended outside the Fibonacci sequence. Various quasi-periodic sequences may be generated by some inflation rules, for example, $A \rightarrow A^mB$, and $B \rightarrow A$ for a class of sequence with two blocks A and B, where A^mB means a sequence of m basic building blocks of type A followed by one block of type B. Some more complex sequences, such as Thue-Morse sequences and fractal sequences, can also be chosen to construct the structures to obtain the required phase-matching wavelength (9). Furthermore, the quasi-periodic structure can also be introduced into nonlinear optical materials that are not ferroelectric. For example, by using some special epitaxial growth method (*12*) or diffusion-bonding technique (*13*), even LiB_3O_5 and β-BaB_2O_4 crystals (*14*), which are widely used for ultraviolet (UV) harmonic generations, with a polar axis changing its direction quasi-periodically might be realized. For a superlattice with a particular material and quasi-periodic sequence type, there is only a finite number of choices for THG with two QPM conditions satisfied simultaneously. However, for a required fundamental wavelength, use of different quasi-periodic structures may be considered, because superlattices with different quasi-periodic modulations can provide different reciprocal vectors for phase matching. In this way, efficient THG might be realized in the UV region (*15*).

Generally speaking, a third harmonic may always generate at any required wavelength as long as structure parameter l satisfies the QPM condition of the sum-frequency process, $\Delta k_2 = 0$, even if $\Delta k_1 \neq 0$ (6). Because the efficiency of the THG depends on the second-harmonic intensity, the smaller the mismatch of the second harmonic, the higher the conversion efficiency of the third harmonic. As long as the chosen structure parameter l of the superlattice makes $\Delta k_2 = 0$, and second-harmonic generation is not severely phase-mismatched or Δk_1 is small, a third harmonic can always be efficiently generated. So, for a given material and quasi-periodic type, the structure parametric l is no longer some fixed value, but may be adjusted in certain regions adjacent to $\Delta k_1 = 0$ in order to get the required frequency of third harmonic. This characteristic is beneficial to the design of a practical third-harmonic device.

Aside from the THG, some other higher-order harmonics can also be generated using the same QPM scheme. For example, the fourth harmonic can be generated by two coupled, cascaded SHG processes. And more interesting effects such as tunable multiwavelength optical parametric oscillation can be expected, where a number of QPM conditions must be satisfied simultaneously. Exploring physical process in various microstructures may offer an opportunity to develop some novel materials with potential applications. We provide an example of possible technical applications of quasi-periodic structure materials in nonlinear optics.

REFERENCES AND NOTES

1. J. D. Joannopoulos, P. R. Villeneuve, S. Fan, *Nature* **386**, 143 (1997).
2. S. He and J. D. Maynard, *Phys. Rev. Lett.* **62**, 1888 (1989).

3. J. A. Armstrong *et al.*, *Phys. Rev.* **127**, 1918 (1962); S. Somkeh and A. Yariv, *Opt. Commun.* **6**, 301 (1972).
4. D. Feng *et al.*, *Appl. Phys. Lett.* **37**, 607 (1980); R. L. Byer, *Nonlinear Opt.* **7**, 234 (1994); V. Pruneri, J. Webjorn, J. Russell, D. C. Hanna, *Appl. Phys. Lett.* **65**, 2126 (1995); S. N. Zhu *et al.*, *Ibid.* **67**, 320 (1995); H. Ito, C. Takyu, H. Inaba, *Electron. Lett.* **27**, 1221 (1991); M. C. Gupta, W. Kozlovesky, A. C. G. Nutt, *Appl. Phys. Lett.* **64**, 3210 (1994); J. D. Bierlein *et al.*, *ibid.* **56**, 1725 (1990).
5. P. J. Steinhardt and S. Ostlund, *The Physics of Quasicrystals* (World Scientific, Singapore, 1997); C. Janot, *Quasicrystals* (Clarendon Press, Oxford, UK, 1992).
6. S. N. Zhu *et al.*, *Phys. Rev. Lett.* **78**, 2752 (1997); Y. Y. Zhu and N. B. Ming, *Phys. Rev. B* **42**, 3676 (1990); J. Feng, Y. Y. Zhu, N. B. Ming, *ibid.* **41**, 5578 (1990).
7. Y. R. Shen, *The Principles of Nonlinear Optics* (Wiley, New York, 1984).
8. For standard Fibonacci sequence, the ratio is $\tau = (1+\sqrt{5})/2$. The ratios other than τ can be derived from other 1D quasi-periodic subclasses. All possible subclasses have been classified [D. Levine and P. J. Steinhardt, *Phys. Rev. B* **34**, 596 (1986)].
9. The blocks *A* and *B* can also be arranged according to other quasi-periodic subclasses and can be composed of one or more layers of different materials [R. Merlin *et al.*, *Phys. Rev. Lett.* **55**, 1768 (1985); A. Behrooz *et al.*, *ibid.* **57**, 368 (1986)].
10. S. N. Zhu *et al.*, *J. Appl. Phys.* **77**, 5481 (1995).
11. Some essential simplifications of the theoretical treatment were considered, including the approximation of slowly varying envelope for fundamental, second-, and third-harmonic fields and ignoring depletion of the fundamental and harmonic field.
12. By using a special deposition method, B. Hadimioglu *et al.* [*Appl. Phys. Lett.* **50**, 1642 (1987)] fabricated multiple-layer ZnO films with the crystallographic orientation changing for alternating layers.
13. L. A. Gordon *et al.*, *Electron. Lett.* **29**, 1942 (1993).
14. H. W. Mao, F. C. Fu, B. C. Wu, C. T. Chen, *Appl. Phys. Lett.* **61**, 1148 (1992).
15. It was reported that $LiTaO_3$ has short-wavelength transparency from 280 nm [K. Mizuuchi, K. Yamamoto, T. Taniuchi, *ibid.* **58**, 2732 (1991)]. Thus, by a suitable choice of a QPOS, harmonic generation in the UV region is possible.
16. We thank D. Feng for stimulating discussions. Supported by a grant for the Key Research Project in Climbing Program from the National Science and Technology Commission of China.

22 May 1997; accepted 22 September 1997

Adiabatic Electron Transfer: Comparison of Modified Theory with Experiment

Stephen F. Nelsen,* Rustem F. Ismagilov, Dwight A. Trieber II

The radical cations of properly designed bishydrazines allow comparison of observed and calculated electron transfer rate constants. These compounds have rate constants small enough to be measured by dynamic electron spin resonance spectroscopy and show charge transfer bands corresponding to vertical excitation from the energy well for the charge occurring upon one hydrazine unit to that for the electron-transferred species. Analysis of the data for all six compounds studied indicates that the shape of the adiabatic surface on which electron transfer occurs can be obtained from the charge transfer band accurately enough to successfully predict the electron transfer rate constant and that explicit tunneling corrections are not required for these compounds.

Reactions in which a single electron is transferred are extremely important in chemistry and biology and have received a great amount of both experimental and theoretical attention since the seminal theoretical work by Marcus in the late 1950s (*1*, *2*). Marcus introduced a method for estimating the barrier ΔG_{et}^{*} for electron transfer (ET) from three parameters: the vertical reorganization energy λ, the electronic interaction matrix element V, and the exothermicity of the reaction $\Delta G°$. In the simplest case (Fig. 1), a $\Delta G° = 0$ reaction, λ is the vertical gap between the minimum on the energy surface of the precursor and the energy surface of the product when neither the solvent nor the internal geometry are allowed to relax. λ is the sum of a solvent contribution (λ_s) and an internal vibrational contribution (λ_v), that is $\lambda = \lambda_s + \lambda_v$. Marcus addressed ways to estimate these quantities (*1*, *2*). The amount of electronic mixing between the precursor and product surfaces is measured by V.

In recent years, most experimental and theoretical studies have concentrated on long-distance ET reactions, which are initiated by photoexcitation (*3*). These reactions have small V and are usually very exothermic. The most important contributions that have emerged from these studies have been the development of vibronic coupling theory to treat such reactions (*4*) and landmark pulse radiolysis studies (*5*) that established the existence of the "inverted region" predicted by Marcus. Such reactions are involved in the charge separation that occurs in photosynthetic reaction centers (*6*), and the development of fast laser kinetic techniques has been crucial in such studies (*3*, *6*). The great majority of biological ET reactions, however, occur in the dark and have small $\Delta G°$. The present work focuses on a series of carefully designed molecules in which ET occurs with $\Delta G° = 0$ and without photoexcitation. These molecules display optical absorption spectra from which λ and V can be estimated, allowing quantitative testing of ET theory.

Symmetrical transition metal–centered intervalence (IV) compounds are conceptually the simplest ET systems and have played a major role in elucidating ET reactions since the first example was prepared in 1969 (*7*). In IV compounds, two metal atoms are connected by a bridging ligand, and the overall charge formally places the metals in different oxidation states. Whether excess charge is delocalized over both metals or localized on one is determined by the relative sizes of λ and V (*7*). If $V < \lambda/2$, then charge localization occurs, and there are separate potential energy wells corresponding to the higher charge being on one metal or the other. These wells are displaced from each other on an ET coordinate X (Fig. 1). If V is large enough, a localized IV compound shows a charge transfer (CT) band, which allows measurement of λ.

Hush developed a simple theory for estimating both λ and V from such IV-CT bands (*8*). Marcus (*1*, *2*) and Hush (*8*) assume that the diabatic energy surfaces (the energy wells in the absence of electronic coupling) are parabolas in a plot of energy versus X. In this case, the transition energy at the IV-CT maximum (E_{op}) is equal to λ. Hush's estimate of V (cm^{-1}), which we shall designate as V_H to distinguish it from other estimates, is

$$V_H = (0.0206/d)(\Delta\nu_{1/2}\varepsilon_{max}E_{op})^{1/2} \quad (1)$$

where d (Å) is the ET distance, $\Delta\nu_{1/2}$ (cm^{-1}) is the IV-CT band width at half-height, and ε_{max} ($M^{-1}cm^{-1}$) is the molar extinction coefficient at the band maximum. Tunneling corrections are also assumed to be necessary to calculate the ET rate constant k_{et} (*1*, *2*, *8*). Estimation of the size of the tunneling correction requires knowing the averaged energy $h\nu_v$ (where h is Planck's constant) of the vibrational frequencies ν_v active in the ET process, which Hush also estimated from the IV-CT band width (*8*).

Symmetrical IV compounds would provide the most direct test of the validity of the ET parameters derived from their IV-CT bands, allowing comparison of the calculated rate constant with the experimental value. Unfortunately no adequate method exists for measuring the large values of k_{et} predicted for transition metal IV compounds (*3*). There is no transient to follow

Department of Chemistry, University of Wisconsin, Madison, WI 53706–1396, USA.

*To whom correspondence should be addressed. E-mail: nelsen@chem.wisc.edu